

- [Circulation Home](#)
- [Subscriptions](#)
- [Archives](#)
- [Feedback](#)
- [Authors](#)
- [Help](#)
- [AHA Journals Home](#)

Circulation. 1996;94:562-570

[« Previous Article](#) | [Table of Contents](#) | [Next Article »](#)

(Circulation. 1996;94:562-570.)

© 1996 American Heart Association, Inc.

Articles

Class III Antiarrhythmic Effects of Zatebradine

Time-, State-, Use-, and Voltage-Dependent Block of hKv1.5 Channels

Carmen Valenzuela, PhD; Eva Delpon, PhD; Laura Franqueza, BS; Pilar Gay, BS; Onesima Perez, PhD; Juan Tamargo, MD, PhD; Dirk J. Snyders, MD

the Institute of Pharmacology and Toxicology, CSIC, School of Medicine, Universidad Complutense, Madrid, Spain, and the Departments of Medicine and Pharmacology, School of Medicine, Vanderbilt University, Nashville, Tenn (D.J.S.).

Correspondence to Carmen Valenzuela, PhD, Institute of Pharmacology and Toxicology, CSIC, School of Medicine, Universidad Complutense, 28040 Madrid, Spain. E-mail carmenva@eucmax.sim.ucm.es.

This Article

- ▶ [Abstract](#) **FREE**
- ▶ [Alert me when this article is cited](#)
- ▶ [Alert me if a correction is posted](#)
- ▶ [Citation Map](#)

Services

- ▶ [Email this article to a friend](#)
- ▶ [Similar articles in this journal](#)
- ▶ [Similar articles in PubMed](#)
- ▶ [Alert me to new issues of the journal](#)
- ▶ [Download to citation manager](#)
- ▶ [Request Permissions](#)

Citing Articles

- ▶ [Citing Articles via HighWire](#)
- ▶ [Citing Articles via Google Scholar](#)

Google Scholar

- ▶ [Articles by Valenzuela, C.](#)
- ▶ [Articles by Snyders, D. J.](#)
- ▶ [Search for Related Content](#)

PubMed

- ▶ [PubMed Citation](#)
- ▶ [Articles by Valenzuela, C.](#)
- ▶ [Articles by Snyders, D. J.](#)
- ▶ [PubMed/NCBI databases](#)
 - [Compound via MeSH](#)
 - [Substance via MeSH](#)

Abstract

Background Zatebradine is a bradycardic agent that inhibits the hyperpolarization-activated current (I_f) in the rabbit sinoatrial node. It also prolongs action potential duration in papillary muscles in guinea pigs and in Purkinje fibers in rabbits. The underlying mechanism by which zatebradine induces this effect has not been explored, but it is likely to involve K^+ channel block.

Methods and Results Cloned human cardiac K^+ delayed rectifier currents (hKv1.5) were recorded in *Ltk*⁻ cells transfected with their coding sequence. Zatebradine 10 $\mu\text{mol/L}$ did not modify the initial activation time course of the current but induced a subsequent decline to a lower steady-state current level with a time constant of 109 ± 16 ms. Zatebradine inhibited hKv1.5 with an apparent K_D of 1.86 ± 0.14 $\mu\text{mol/L}$. Block was voltage dependent (electrical distance $\delta = 0.177 \pm 0.003$) and accumulated in a use-dependent manner during 0.5- and 1-Hz pulse trains because of slower recovery kinetics in the presence of the drug. Zatebradine reduced the tail current

- ▲ [Top](#)
- [Abstract](#)
- ▼ [Introduction](#)
- ▼ [Methods](#)
- ▼ [Results](#)
- ▼ [Discussion](#)
- ▼ [References](#)

amplitude, recorded at -30 mV, and slowed the deactivation time course, which resulted in a "crossover" phenomenon when control and zatebradine tail currents were superimposed.

Conclusions These results indicate that (1) zatebradine is an open-channel blocker of hKv1.5, (2) binding occurs in the internal mouth of the ion pore, (3) unbinding is required before the channel can close, and (4) zatebradine-induced block is use dependent because of slower recovery kinetics in the presence of the drug. These effects may explain the prolongation of the cardiac action potential and could be clinically relevant.

Key Words: heart rate • antiarrhythmia agents • potassium • action potentials

Introduction

Sinus tachycardia is a common physiological response that maintains homeostasis by increasing cardiac output. However, an increased heart rate increases myocardial oxygen demand and decreases time for myocardial relaxation and diastolic ventricular filling.¹ In the presence of a flow-limiting coronary artery stenosis, a decrease in diastolic perfusion time secondary to exercise-induced tachycardia may be deleterious because it further reduces subendocardial blood flow.^{2 3} Under these circumstances, drugs that block sinus tachycardia, reduce heart rate at rest, or both could be expected to reduce myocardial oxygen demand and to increase the diastolic coronary perfusion time, thus improving perfusion and function of the ischemic subendocardium.^{2 4 5}

- ▲ [Top](#)
- ▲ [Abstract](#)
- [Introduction](#)
- ▼ [Methods](#)
- ▼ [Results](#)
- ▼ [Discussion](#)
- ▼ [References](#)

Zatebradine (UL-FS 49 Cl) {1,3,4,5-tetrahydro-7,8-dimethoxy-3-[3-[[2-(3,4-dimethoxyphenyl)ethyl]methylimino]propyl]-2H-3-benzazepin-2-on hydrochloride} is a specific bradycardic agent⁶ that blocks sinus tachycardia and markedly attenuates exercise-induced heart rate both in animal models^{7 8 9 10} and in humans^{11 12 13 14} at concentrations that do not affect the inotropic or lusitropic state or the vascular tone. Therefore, it may offer a new therapeutic perspective in the treatment of effort-induced angina pectoris, particularly in patients with depressed left ventricular function.

The precise mechanism of the bradycardic effect of zatebradine is still uncertain. In rabbit sinoatrial node cells¹⁵ and sheep Purkinje fibers,^{16 17} the bradycardic effect of zatebradine has been attributed to a use-dependent inhibition of the hyperpolarization-activated current (I_f) that apparently is caused by interaction with the open state of the channel. At the same concentrations, zatebradine has minimal effects on the L-type Ca^{2+} current (I_{Ca}) or the delayed rectifier K^+ current (I_{Kr}) in rabbit sinoatrial cells.¹⁵ However, in spontaneously beating rabbit sinoatrial cells, zatebradine prolonged the duration of the action potential.^{15 18} More recent electrophysiological studies demonstrated that zatebradine also prolongs action potential duration in guinea pig papillary muscles^{19 20} and rabbit Purkinje fibers,¹⁹ an effect that was more prominent in Purkinje fibers than in papillary muscles. This prolongation (class III action) by zatebradine likely is due to its ability to block an outward K^+ current that is different from the I_{Kr} present in rabbit sinoatrial myocytes.

In human cardiomyocytes, K^+ currents that are activated by depolarization have been identified as transient outward currents (I_{to})^{21 22 23 24} and delayed rectifier currents with rapid (I_{Kr}) and slow (I_{Ks}) components.²⁵ More recently, a very rapidly activating delayed rectifier current (I_{Kur}) was observed in dog ventricle,²⁶ rat atria,²⁷ and adult human atria.²⁸ The biophysical and pharmacological characteristics of I_{Kur} are similar to those reported for the cloned cardiac hKv1.5 channel, which suggests that it is the native counterpart to hKv1.5 channels cloned from human ventricle.^{26 27 28 29 30 31} In addition, the presence of hKv1.5 has been demonstrated in human myocardium by use of immunohistological techniques.³² Block of cardiac K^+ channels has been considered to be the mechanism by which class III antiarrhythmic drugs slow repolarization and prolong the action potential duration.^{33 34 35} Different voltage-gated K^+ currents are involved in the repolarization of human cardiac action potential, including I_{Ks} , I_{Kr} , I_{to} , and I_{Kur} .^{21 22 23 24 25} Importantly, selective block of the hKv1.5-like current in human atrial myocytes results in significant prolongation of the action potential duration,²⁸ and therefore it represents a potential molecular target for class III antiarrhythmic drugs.³⁶

In the present study, we used a stable, heterologous Kv1.5 expression system to determine the mechanism of action of zatebradine in detail without the complications of overlapping currents and limited availability of human tissue. A preliminary report of this study has been published in abstract form.³⁷

Methods

Transfection and Cell Culture

The stable L-cell line expressing hKv1.5 has been described previously.³⁰ The expression vector contains a dexamethasone-inducible, murine mammary-tumor virus promoter that controls transcription of the inserted cDNA and a gene that confers

neomycin resistance driven by the SV40 early promoter; the latter maintains selection against cells that would drop the construct. The cell line used for the experiments reported in the present study displayed hKv1.5-specific mRNA expression after dexamethasone induction as evidenced by Northern blot analysis.²⁹ In addition, the presence of the hKv1.5 protein was demonstrated by Western blot analysis and immunostaining.³² Transfected cells were cultured in DMEM supplemented with 10% horse serum and 0.25 mg/mL G418 (a neomycin analog) under a 5% CO₂ atmosphere. The cultures were passed every 3 to 5 days by use of a brief trypsin treatment. Before experimental use, subconfluent cultures were incubated with 2 μmol/L dexamethasone for 24 hours to induce expression of hKv1.5 channels. The cells were removed from the dish with a rubber policeman, a procedure that left the vast majority of the cells intact. The cell suspension was stored at room temperature (20°C to 22°C) and used within 12 hours for all the experiments reported here.

▲ Top
▲ Abstract
▲ Introduction
■ Methods
▼ Results
▼ Discussion
▼ References

Electrophysiological Recording

Experiments were performed in a small-volume (0.5-mL) bath mounted on the stage of an inverted microscope (Nikon model TMS). An aliquot of cell suspension was transferred into the bath, and the cells were allowed to adhere to the bottom for 15 minutes, at which time the chamber was perfused continuously at a flow rate of 0.5 to 1.0 mL/min. Bath temperature was maintained at 25.0±0.5°C.

The recording chamber contained a silver–silver chloride electrode connected to the CV-3 headstage of the Axopatch-1C voltage-clamp amplifier and Labmaster TL-1 DMA interface (Axon Instruments). The hKv1.5 current was measured by use of the whole-cell voltage-clamp configuration of the patch-clamp technique.³⁸ Micropipettes were pulled from borosilicate glass capillary tubes (Narishige, GD-1) on a P-87 programmable horizontal puller (Sutter Instrument) and heat polished with a microforge (Narishige). The micropipettes were filled with intracellular solution (see "Solutions") filtered through a micropore filter. Current records were sampled at 3 to 10 times the antialias filter setting and stored on the hard disk of a Hewlett Packard Vectra 486/33VL computer for subsequent analysis. Data acquisition and command potentials were controlled by use of PCLAMP 5.5.1. software (Axon Instruments). To ensure voltage-clamp quality, micropipette resistance was kept between 2 and 4 MΩ. The microelectrodes were gently lowered onto the cells to obtain a gigaohm seal (16±6 GΩ; n=20) after suction was applied. After seal formation, cells were lifted from the bottom of the perfusion bath, and the membrane patch was ruptured with brief additional suction. The capacitive transients elicited by symmetrical 10-mV steps from -80 mV were digitized at 50 kHz (filtered at 10 to 20 kHz) for subsequent calculation of cell capacitance (21±2 pF; n=20) and uncompensated access resistance (7±2 MΩ; n=20). Thereafter, capacitance and series resistance compensation were optimized, and 80% compensation of the effective access resistance was usually obtained.

Solutions

The intracellular pipette-filling solution contained (in mmol/L) potassium-aspartate 80, KCl 50, KH₂PO₄ 10, MgATP 3, HEPES 10, and EGTA 5 and was adjusted to pH 7.25 with KOH. The bath solution contained (in mmol/L) NaCl 130, KCl 4, CaCl₂ 1.8, MgCl₂ 1, HEPES 10, and glucose 10 and was adjusted to pH 7.35 with NaOH. Zatebradine as a powder was kindly supplied by Dr Yves Joulin (Institut de Recherches Internationales Servier, Paris, France). The drug was added to the external solution from a stock solution (10⁻² or 10⁻³ mol/L) in distilled, deionized H₂O.

Pulse Protocol and Analysis

After control data were obtained, bath perfusion was switched to drug-containing solution. The holding potential was maintained at -80 mV. Drug infusion or removal was monitored with test pulses from -80 mV to +30 mV applied every 30 seconds until steady state was obtained (within 10 to 15 minutes). The cycle time for any protocol was 10 seconds to avoid accumulation of block or an incomplete reactivation of the current.

The protocol to obtain I-V relationships and activation curves consisted of 500-ms depolarizing pulses that were imposed in 10-mV increments between -80 and +60 mV with additional interpolated pulses to yield 5-mV increments between -30 and +10 mV (activation range of hKv1.5).³⁰ The steady-state I-V relationships were obtained by measuring the current at the end of the 500-ms depolarizations. Between -80 and -40 mV, only passive linear leak was observed, and least-squares fits to these data were used for passive leak correction. Deactivating tail currents were recorded on return to -30 mV. The activation curve was obtained from the tail current amplitude immediately after the capacitive transient. Measurements were made by use of the CLAMPFIT program of PCLAMP 5.5.1. and a custom-made analysis program. Activation curves were fitted with a Boltzmann equation

$$y = \frac{1}{1 + \exp[-(E - E_h)/s]} \quad (E1)$$

in which *s* represents the slope factor; *E*, the membrane potential; and *E_h*, the voltage at which 50% of the channels are open. The time course of tail currents and the slow inactivation were fitted with the sum of exponentials. The activation kinetics were determined with the dominant time constant of activation approach, in which a single exponential was fitted to the latter 50% of activation.^{30 39 40} The curve-fitting procedure used a nonlinear least-squares (Gauss-Newton) algorithm. Results were displayed in linear and semilogarithmic format together with the difference plot. Goodness of fit was judged by the χ^2 criterion and by inspection for systematic nonrandom trends in the difference plot. The same approach was used to fit the use-dependent onset of block and the recovery kinetics.

A first-order blocking scheme was used to describe drug-channel interaction. The apparent affinity constant, K_D , and Hill coefficient, n_H , were obtained from fitting of the fractional block, f , at various drug concentrations with the equation

$$f=1/[1+(K_D/[D])^{n_H}] \quad (\text{E2})$$

and apparent rate constants for binding (k) and unbinding (l) were obtained from fitting the equation

$$k \times [D] + l = 1/\tau_B \quad (\text{E3})$$

Voltage dependence of block was determined as follows: leak-corrected current in the presence of drug was normalized to matching control to yield fractional block at each voltage ($f=1-I_{\text{drug}}/I_{\text{control}}$). The voltage dependence of block was fitted with the equation

$$f=[D]/\{[D]+K_D \times \exp(-\delta z F E / R T)\} \quad (\text{E4})$$

where z , F , R , and T represent valence, Faraday's constant, gas constant, and absolute temperature, respectively. The δ value represents the fractional electrical distance, ie, the fraction of the transmembrane electrical field sensed by a single charge at the receptor site, and K_D^* represents the apparent K_D at the reference membrane potential (0 mV).

Statistical Methods

Results are expressed as mean \pm SEM. Direct comparisons between mean values in control conditions versus mean values in the presence of drug for a single variable were performed by use of a paired Student's t test. ANOVA was used to compare more than two groups. A value of $P < .05$ was considered significant.

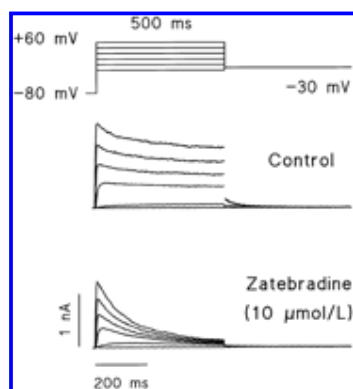


Results

Dose-Dependent and Reversible Block by Zatebradine

The top panel of Fig 1 shows superimposed original records of hKv1.5 in expressed *Ltk*⁻ cells after the application of 500-ms depolarizing pulses from a holding potential of -80 mV to different test potentials between -40 and +60 mV. Under control conditions, the outward K⁺ current rose rapidly with a sigmoidal time course to a peak and then declined slowly (slow and partial inactivation). The activation time constant was 0.90 \pm 0.13 ms at +60 mV ($n=6$). Outward tail currents were observed on repolarization to -30 mV that exhibited a time constant of deactivation of 53 \pm 13 ms. These results are similar to previous reports^{30 31 41} of functional properties of hKv1.5 expressed in L cells. The bottom panel of Fig 1 shows that zatebradine 10 $\mu\text{mol/L}$ did not modify the activation time constant (1.05 \pm 0.14 ms at +60 mV; $n=5$; $P > .05$). However, it reduced the peak outward potassium current modestly and induced a prominent decline that reached steady-state values at the end of a 500-ms pulse. This decline occurred much more quickly and to a greater extent than the slow inactivation observed in control conditions and therefore could be well separated from the intrinsic slow and partial inactivation observed under control conditions. Furthermore, a similar percentage of block was observed after 1-second duration pulses. When hKv1.5 block was measured at the end of a 500-ms pulse from -80 to +60 mV, zatebradine 10 $\mu\text{mol/L}$ reduced the hKv1.5 current by 82 \pm 3% ($n=7$). After perfusion was switched with zatebradine, induction of block progressed with a time constant of 3 to 4 minutes, which was about five times slower than the effect of changing extracellular K⁺ concentration at similar flow rates. This suggested an intramembrane or intracellular site of action, and therefore 15 minutes of equilibration was allowed to elapse before drug effects were assessed. The effects were reversible on washout of the drug. In 20 cells, the current was restored to 88 \pm 2% of its initial control value after perfusion with drug-free solution over a 20-minute period.

- [▲ Top](#)
- [▲ Abstract](#)
- [▲ Introduction](#)
- [▲ Methods](#)
- [■ Results](#)
- [▼ Discussion](#)
- [▼ References](#)



View larger version (19K):
[\[in this window\]](#)

Figure 1. Effects of zatebradine (10 $\mu\text{mol/L}$) on hKv1.5. Currents are shown for depolarizations from -80 mV to voltages between -40 and +60 mV in steps of 20 mV. Tail currents were obtained on return to -30 mV. Top, traces obtained under control conditions; Bottom, traces recorded in the presence of zatebradine 10 $\mu\text{mol/L}$. Cell capacitance, 21 pF. Data filtered at 2 kHz (four-pole Bessel) and digitized at 10 kHz; additional digital filtering at 1 kHz.

[\[in a new window\]](#)

Fig 2⁺ shows the concentration dependence of zatebradine-induced block of hKv1.5 measured at the end of 500-ms depolarizing pulses from -80 to +60 mV. In the presence of zatebradine, block averaged $21 \pm 5\%$ ($n=5$) at $0.5 \mu\text{mol/L}$, $53 \pm 3\%$ ($n=6$) at $2 \mu\text{mol/L}$, $82 \pm 3\%$ ($n=7$) at $10 \mu\text{mol/L}$, and $94 \pm 3\%$ ($n=4$) at $20 \mu\text{mol/L}$. A nonlinear least-squares fit of the concentration-response equation (Equation 2 in "Methods") to the individual data points yielded an apparent K_D of $1.86 \pm 0.14 \mu\text{mol/L}$ and an n_H of 0.97 ± 0.06 . The dashed line in Fig 2⁺ illustrates a fit to the same data with the n_H fixed to 1; the apparent K_D value obtained for zatebradine was similar to that obtained without constraint of the n_H . This coefficient, which is close to unity, suggests that binding of one zatebradine molecule per channel is enough to block K^+ permeation.

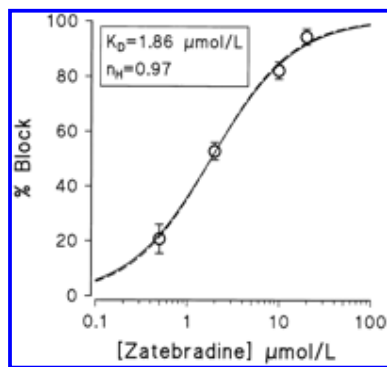


Figure 2. Concentration dependence of zatebradine-induced block of hKv1.5. Reduction of current (relative to control) at the end of 500-ms depolarizations to +60 mV was used as index of block. Data are mean \pm SEM of a total of 20 experiments. The continuous line represents the fit of the experimental data to the equation $1 / \{1 + (K_D/[D])^{n_H}\}$. For comparison, the dashed line represents the fit for a Hill coefficient (n_H) of 1.

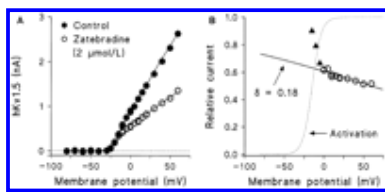
View larger version (17K):

[\[in this window\]](#)

[\[in a new window\]](#)

Voltage-Dependent Block by Zatebradine of hKv1.5 Channels

Fig 3A⁺ shows the effects of $2 \mu\text{mol/L}$ zatebradine on the steady-state I-V relationship for the hKv1.5 channel. Cells were held at -80 mV, and 500-ms depolarizing pulses were applied in steps of 10 mV to different potentials from -80 mV to +60 mV, with the exception of membrane potentials between -30 and +10 mV, in which depolarizing pulses were applied in 5-mV steps because this voltage range corresponds to the slope of the activation curve of the current. The I-V relationship under control conditions was almost linear for depolarizations positive to +10 mV, and the sigmoidicity between -30 and +10 mV reflects the voltage dependence of channel gating.^{30 31} In the presence of zatebradine $2 \mu\text{mol/L}$, the curve displayed a downward curvature at test potentials positive to 0 mV, which suggested that this drug produced more block at very positive depolarizations. To quantify this voltage dependence of hKv1.5 block, the relative current $I_{\text{zatebradine}}/I_{\text{control}}$ was plotted as a function of membrane potential (Fig 3B⁺) together with the activation curve. The hKv1.5 block increased steeply between -30 and 0 mV, which corresponds to the voltage range of channel opening. These data suggest that zatebradine preferentially binds to the open state of the channel. Between 0 and +60 mV, block continued to increase with a more shallow voltage dependence, although hKv1.5 activation had reached saturation over this voltage range (Fig 3B⁺). For instance, with zatebradine $2 \mu\text{mol/L}$, the degree of block increased in a voltage-dependent manner from $43.7 \pm 3.4\%$ at 0 mV to $52.9 \pm 3.3\%$ at +60 mV ($n=6$). Paired analysis in six experiments with zatebradine $2 \mu\text{mol/L}$ indicated that this voltage-dependent increase in block was significant (difference, $9.1 \pm 1.5\%$; $P < .01$). Zatebradine is a weak base and has a tertiary amine group with $\text{p}K_a = 8.73$,⁴² and thus, this drug will be predominantly present (99.5%) in its cationic form at the intracellular pH of 7.25. Therefore, the shallow voltage dependence of block at potentials positive to 0 mV could be due to the effect of the transmembrane electrical field on the interaction between the zatebradine ion and the channel receptor.^{30 41} If zatebradine reaches the receptor from the inside, then channel block is expected to increase in a voltage-dependent manner according to a Boltzmann relationship (Equation 4 in "Methods"). The parameter δ in this equation represents the fractional electrical distance, ie, the fraction of the membrane electrical field sensed by a single charge at the receptor site. Fig 3B⁺ shows the fit of this equation to data points positive to 0 mV, with a δ of 0.18 for this particular experiment. In six experiments with zatebradine $2 \mu\text{mol/L}$, the average value for δ was 0.177 ± 0.002 .



View larger version (16K):

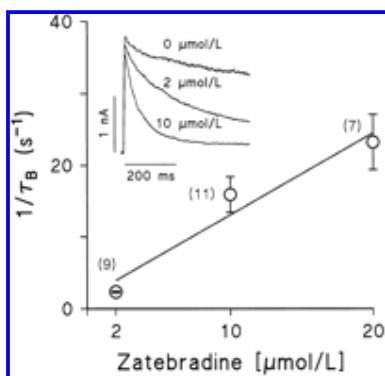
[\[in this window\]](#)

[\[in a new window\]](#)

Figure 3. Voltage dependence of hKv1.5 block by zatebradine (2 $\mu\text{mol/L}$). A, Current-voltage relationship (500 ms isochronal) in control and in the presence of zatebradine 2 $\mu\text{mol/L}$. B, Relative current expressed as $I_{\text{zatebradine}}/I_{\text{control}}$ from data shown in Fig 3A. The dashed line represents the activation curve for this experiment. Block increased steeply between -20 and 0 mV (\blacktriangle), which corresponds to the voltage range of activation of hKv1.5. For membrane potentials positive to 0 mV, a continued but more shallow voltage dependence was observed (\circ). This voltage dependence was fitted (continuous line) with use of Equation 4 (see "Methods") and yielded $\delta=0.18$.

Concentration Dependence of Time Course of Channel Block

If zatebradine can access its receptor site only when the hKv1.5 channel is opened, then the inhibition of the potassium current would develop only when the channels start to open, and development of block should be visible during a 500-ms depolarizing step if the blocking rate is slower than the opening rate. On the other hand, if the blocking rate exceeded that of channel opening or if zatebradine blocked other states of the channel, the current recorded in the presence of drug would be expected to be scaled down. Fig 4 shows superimposed recordings of 500-ms depolarizations from -80 to +60 mV in the absence and presence of zatebradine 2 and 10 $\mu\text{mol/L}$. Under control conditions, the potassium current reached its maximum peak within 10 ms and then declined slowly, with a time constant of 160 ms (partial slow inactivation). However, in the presence of zatebradine, the subsequent time course displayed an additional exponential component superimposed on the slow inactivation that can be separated from the slow inactivation at concentrations $\geq 10 \mu\text{mol/L}$. The decline of the current in the presence of zatebradine 2 $\mu\text{mol/L}$ was very slow; thus, the kinetics of development of block at this concentration was assessed by use of a double-pulse protocol in which a conditioning pulse of variable duration (from 10 to 5000 ms) to +60 mV was followed by a test pulse of 30 ms to +60 mV. This pulse protocol allowed us to separate the slow inactivation from the development of block in the presence of this low concentration of zatebradine. The current values measured at the end of the test pulse were plotted versus the time of the conditioning pulse and fitted by a monoexponential function that yielded a time constant of block of 434.5 ± 18.0 ms ($n=9$). The time constants of the fast component in the presence of zatebradine 10 and 20 $\mu\text{mol/L}$ were 109.2 ± 16.3 ($n=7$) and 52.5 ± 9.7 ms ($n=7$), respectively. These time constants (τ_B), together with that obtained with the double-pulse protocol for zatebradine 2 $\mu\text{mol/L}$, can be taken as an approximation of the drug-channel interaction kinetics.^{30 41} Fig 4 shows the concentration dependence of τ_B ($n=7$ to 11 experiments at each concentration). Fig 4 also shows the least-squares fit with the relation $1/\tau_B = kx[D] + l$ (see "Methods"). From this fit, the following values for the apparent association (k) and dissociation rate constants (l) were obtained: $k = (1.14 \pm 0.27) \times 10^6$ ($\text{mol/L})^{-1} \cdot \text{s}^{-1}$ and $l = (1.63 \pm 3.55) \text{ s}^{-1}$, respectively. From these values, an apparent $K_D (=l/k)$ of 1.4 $\mu\text{mol/L}$ can be calculated, which is very close to the K_D of 1.8 $\mu\text{mol/L}$ obtained from the steady-state inhibition shown in Fig 2.



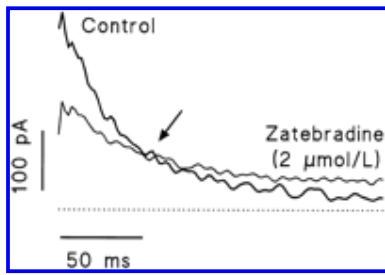
View larger version (18K):

[\[in this window\]](#)

[\[in a new window\]](#)

Figure 4. Kinetics of block induction by zatebradine during a single 500-ms depolarizing pulse from -80 to +60 mV. Rate of block as function of concentration. The time constant of the zatebradine-induced fast component (τ_B) was obtained from biexponential fits to the falling phase of the tracings in the inset. The $1/\tau_B$ values were plotted vs drug concentration. For a first-order blocking scheme, a linear relation is expected: $1/\tau_B = kx[D] + l$. The solid line represents the fit from which the apparent binding and unbinding rate constants were obtained. Inset, Superimposed traces for steps from -80 to +60 mV under control conditions and in the presence of zatebradine 2 and 10 $\mu\text{mol/L}$. In the presence of zatebradine, the current activated initially as under control conditions but reached a lower peak and subsequently declined more quickly.

The hKv1.5 currents deactivated completely at -30 mV with a time constant of 53 ± 13 ms ($n=6$). This time constant reflects primarily the virtually irreversible closing of the channel. If zatebradine binds only to the open state of the potassium channel, then the dissociation of zatebradine from the blocked channel results in an open channel, which subsequently could close. Blocked channels are not conducting, and the conversion to open channels should result in a slower decline of the tail current because some fraction of the open channels become blocked again rather than closing irreversibly. Fig 5 shows the superposition of the tail currents obtained at -30 mV after 500-ms depolarization to +60 mV under control conditions and in the presence of zatebradine 2 $\mu\text{mol/L}$. After exposure to drug, the amplitude of the tail current was decreased and its time course slowed from 53 ± 13 to 97 ± 17 ms ($n=6$; $P < .05$). These results further support an open-channel interaction between zatebradine and the hKv1.5 channels.



View larger version (13K):

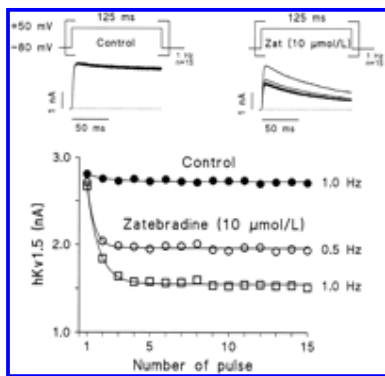
[\[in this window\]](#)

[\[in a new window\]](#)

Figure 5. Tail current crossover between the tail current recorded under control conditions and in the presence of zatebradine 2 $\mu\text{mol/L}$. Tail currents were obtained at -30 mV after a 500-ms depolarizing pulse to $+60$ mV. Arrow indicates crossover of the trace recorded in the presence of zatebradine with the trace recorded under control conditions. The dotted line represents the zero level of current.

Use-Dependent Block of hKv1.5 Channels by Zatebradine

Although zatebradine 2 $\mu\text{mol/L}$ induced over 50% steady-state block, this amount of block may not be attained during a single action potential. Therefore, we tested whether zatebradine-induced block displayed use dependence. Trains of 15 depolarizing pulses of 125-ms duration from -80 mV to $+50$ mV were applied at two different stimulation frequencies, 0.5 and 1 Hz. Fig 6 shows original current records obtained after such pulse train was applied at a frequency of 1 Hz in the absence and presence of zatebradine 10 $\mu\text{mol/L}$. Under control conditions, the outward K^+ current displayed little decline. In the presence of zatebradine 10 $\mu\text{mol/L}$, the size of the current decayed progressively until it reached a steady-state block after approximately 4 depolarizing pulses. Fig 6 also shows the effects of these pulse trains on the maximal peak currents elicited during the application of these pulse protocols in the absence and presence of zatebradine 10 $\mu\text{mol/L}$. Under control conditions, the maximal peak current decayed by $9\pm 2\%$ ($n=4$) and $10\pm 3\%$ ($n=4$) after application of trains of depolarizing pulses from -80 mV to $+50$ mV at 0.5 and 1.0 Hz, respectively. In the presence of zatebradine 10 $\mu\text{mol/L}$, there was a statistically significant use-dependent block at both frequencies of stimulation that averaged $30\pm 3\%$ ($P<.01$; $n=4$) and $44\pm 3\%$ ($P<.01$; $n=4$) at 0.5 Hz and 1.0 Hz, respectively. The analysis of this exponential decay yielded rate constants of 1.5 ± 0.1 ($n=4$) and 1.0 ± 0.3 pulse $^{-1}$ ($n=4$) at 0.5 and 1.0 Hz, respectively. This use-dependent inhibition of hKv1.5 current was concentration dependent. Therefore, after application of a train of 15 depolarizing pulses from -80 mV to $+50$ mV at a frequency of 1 Hz in the presence of 2 $\mu\text{mol/L}$ zatebradine, a $20\pm 2\%$ inhibition of the current was observed ($n=4$; $P<.01$). When the current inhibition was measured at the end of the 125-ms depolarizing pulses at 0.5 and 1 Hz in the absence and presence of zatebradine 10 $\mu\text{mol/L}$, the values obtained were $9\pm 2\%$ versus $35\pm 4\%$ ($P<.01$; $n=4$) and $9\pm 3\%$ versus $42\pm 5\%$ ($P<.01$; $n=4$), respectively.



View larger version (26K):

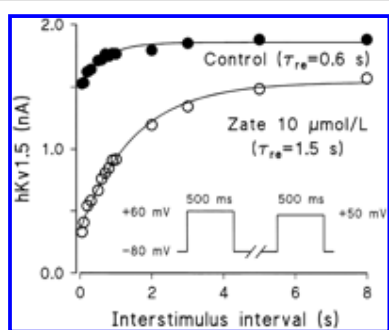
[\[in this window\]](#)

[\[in a new window\]](#)

Figure 6. Use-dependent block of hKv1.5 induced by zatebradine 10 $\mu\text{mol/L}$. Top, Original records obtained after application of a train of depolarizing pulses of 125 ms in duration from -80 to $+50$ mV under control conditions (left) and in the presence of zatebradine 10 $\mu\text{mol/L}$ (Zat) (right). The dotted line represents the zero level of current. Bottom, Outward hKv1.5 peak current amplitude in control conditions and in the presence of zatebradine 10 $\mu\text{mol/L}$ during trains of 15 depolarizing pulses (125 ms in duration) from -80 to $+50$ mV at a frequency of 1 Hz in control conditions (*) and at 0.5 (○) and 1.0 Hz (□) in the presence of zatebradine.

These results indicated that block of hKv1.5 channels by zatebradine increased as the frequency of stimulation was augmented and could be explained if the recovery process of blocked channels ($\text{OZ} \rightarrow \text{O} \rightarrow \text{C}$) was slower than the transition between the open (O) and the closed (C) state in the absence of drug (Z). To explore this possibility, we determined the kinetics of the recovery process using the following experimental protocol: a conditioning prepulse of 500-ms duration from -80 to $+60$ mV was followed by a fixed test pulse of 500-ms duration to $+50$ mV after an interstimulus interval of variable duration (between 50 and 8000 ms) at -80 mV. Fig 7 shows a typical example of the recovery kinetics of hKv1.5 current (measured as the maximal peak current) obtained in both the absence and presence of zatebradine 10 $\mu\text{mol/L}$. Under control conditions, the recovery process of the hKv1.5 current was defined by a monoexponential process that exhibited a time constant (τ_{re}) of 0.8 ± 0.2 seconds ($n=4$). In the presence of zatebradine 10 $\mu\text{mol/L}$, this recovery was also monoexponential, but τ_{re} increased to 1.6 ± 0.2 seconds ($P<.05$; $n=4$). The slower recovery kinetics of the hKv1.5 current can explain the use-dependent block induced by zatebradine during the application of

trains of depolarizing pulses, since after interstimulus intervals of 1 and 2 seconds, there was still an accumulated percentage block of $45\pm 2\%$ and $27\pm 2\%$, respectively.



View larger version (21K):

[\[in this window\]](#)

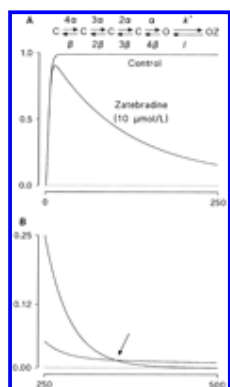
[\[in a new window\]](#)

Figure 7. Recovery process of hKv1.5 current under control conditions and in the presence of zatebradine $10\ \mu\text{mol/L}$ (Zate). The graph shows the maximum peak amplitude of outward hKv1.5 currents elicited by a test pulse as a function of the time interval in the absence (\bullet) and presence (\circ) of zatebradine $10\ \mu\text{mol/L}$. Continuous lines represent the best monoexponential fit of the increase of hKv1.5 currents as a function of the interstimulus interval from which τ_{re} was obtained as indicated in the figure.

Mathematical Modeling

The experimental results obtained in the present study were interpreted and simulated by use of a kinetic-state diagram similar to those used for the related *Drosophila* Shaker and rat brain RCK1 (Kv1.1) voltage-gated potassium channels⁴³ and that was previously described for this hKv1.5 channel.^{31 41}

A simple way to incorporate the interaction of zatebradine into this diagram is to assume that the drug binds to the open state of the channel, as indicated in the scheme. Since the activation process is fast, at potentials positive to $0\ \text{mV}$, this system functionally reduces to a three-pool model ($I \rightleftharpoons O \rightleftharpoons OZ$). In the presence of zatebradine, the inactivation became biexponential, as expected for this model. The drug-induced extra component of inactivation had a time constant that was much faster than that of the slow inactivation of the current under control conditions. Therefore, this fast time constant ($1/\tau_B = kx[D] + l$) can be considered to represent the interaction of zatebradine with the open state of the hKv1.5 channel ($O \rightleftharpoons OZ$). Fig 8⁴ shows the result of a mathematical simulation of the effects of zatebradine at $10\ \mu\text{mol/L}$ based on this open-channel block model. The voltage dependence of the drug-channel interaction was incorporated, but inactivation was omitted for simplicity. When the rate constants obtained for the drug-channel interaction were used, the simulation reproduced the experimental results fairly well, consistent with the proposed open-channel block mechanism.



View larger version (13K):

[\[in this window\]](#)

[\[in a new window\]](#)

Figure 8. Mathematical modeling of zatebradine interactions with hKv1.5 channels. The open-channel block model was used with the following rate constants: at $+60\ \text{mV}$, $\alpha = 400\ \text{s}^{-1}$, $\beta = 1\ \text{s}^{-1}$, $k = 1.1\ (\mu\text{mol/L})^{-1}\cdot\text{s}^{-1}$, and $l = 1.6\ \text{s}^{-1}$; at $-30\ \text{mV}$, $\alpha = 0.1\ \text{s}^{-1}$, $\beta = 7\ \text{s}^{-1}$, $k = 0.7\ (\mu\text{mol/L})^{-1}\cdot\text{s}^{-1}$, and $l = 2.6\ \text{s}^{-1}$. A, Mathematical simulations for maximal outward currents elicited during 250-ms steps from -80 to $+60\ \text{mV}$. B, Mathematical simulations for tail currents elicited during a 250-ms step to $-30\ \text{mV}$ applied after a 250-ms step to $+60\ \text{mV}$. Arrow indicates tail current crossover. Currents for step and tail were scaled to reflect the difference in driving force.

Discussion

The main findings of the present study were as follows: (1) the charged form of zatebradine bound to the open state of hKv1.5 channels; (2) binding occurred within the transmembrane electrical field and was described by a fractional electrical distance (δ) of 0.18; (3) zatebradine-induced block was use dependent; (4) the use-dependent block was due to a slow

recovery from block in the presence of drug; and (5) unbinding was required before the channel could close. The K_D for hKv1.5 block is only fourfold higher than that for use-dependent I_f inhibition in rabbit sinoatrial node cells,¹⁵ which suggests that this class III action may have clinical relevance.

Zatebradine Binds to the Open State of the hKv1.5 Channel

The block of hKv1.5 channels induced by zatebradine displayed time-, state-, and voltage-dependent interactions. In the presence of this drug, (1) there were no changes in the activation kinetics, (2) the block developed after channels opened and increased steeply in the voltage range of channel opening, and (3) a "crossover" phenomenon in the tail currents was observed. All these data strongly suggested an interaction of zatebradine with the open state of the hKv1.5 channel. The assumption that the fast component represented the $O \rightleftharpoons OZ$ transition did not apply at low drug concentrations, because the time constant of block was similar to that of slow inactivation. Therefore, we needed to use a double-pulse protocol to extract the kinetic information. The apparent binding and unbinding rate constants for zatebradine were calculated to be $k=(1.14 \pm 0.27) \times 10^6 (\text{mol/L})^{-1} \cdot \text{s}^{-1}$ and $l=(1.63 \pm 3.55) \text{ s}^{-1}$. From these rate constants, the apparent affinity ($K_D=l/k$) was estimated to be $1.4 \mu\text{mol/L}$. This estimate is in good agreement with the value obtained from steady-state suppression of the hKv1.5 current ($1.86 \mu\text{mol/L}$). This agreement between both independent methods to estimate the affinity further supports the open-channel block model used to derive the rate constants.

Voltage Dependence of Zatebradine Block

Zatebradine is a weak base, with a pK_a of 8.73⁴²; therefore, 99.5% of the drug is in its charged form at pH 7.4, and 0.5% is in its neutral form. Access of the hydrophilic (charged) form of the drug to the receptor site requires a hydrophilic pathway.^{42, 44} This mode of access most likely requires that the charged drug move into the electrical membrane field. This provides an additional attraction to or repulsion from the receptor. Depolarization will promote the entry of a cationic drug from the inside into the channel, whereas hyperpolarization will decrease it. This interaction can be considered to change the drug concentration at the receptor site in a voltage-dependent manner or to modify the receptor affinity because it adds a voltage-dependent term to the rate constants of drug binding and unbinding. If a drug has a high affinity for activated and/or open channels, the voltage dependence of channel activation is superimposed on the intrinsic voltage dependence of drug binding because channel activation makes the receptor available. The total voltage dependence of block is then composed of a steep phase that reflects channel activation and a shallower phase that reflects the additional effect of the electrical field on the charged drug (see Fig 3B). Therefore, the δ value of 0.18 observed in the presence of zatebradine for the voltage dependence of the apparent K_D can be interpreted to indicate that the positively charged zatebradine senses 18% of the membrane electrical field. It is of interest to note that the time constant of recovery from block at -80 mV was 1.5 seconds, ie, similar to the dissociation rate constant (l) obtained at +60 mV ($\tau_{re}=0.6$ seconds from $l=1.6 \text{ s}^{-1}$). This indicates that the rate of dissociation displays no significant voltage dependence. This suggests that the drug is not trapped in the channel on hyperpolarization, because in that case we would expect much different values between potentials where the channel is open (+60 mV) or closed (-80 mV), and that the voltage dependence of block likely resides in the association rate constant (k) and not in the dissociation rate constant (l), which only decreases 2.6-fold, from -80 mV to +60 mV.

Receptor Site for Zatebradine on hKv1.5

The voltage dependence observed in the presence of zatebradine strongly suggests that the binding site is located within the membrane electrical field. In other words, the receptor site for zatebradine is located in the membrane spannings of the hKv1.5 channel. The amino acid sequence 462 to 480 of hKv1.5 is identical to this "pore" sequence of the related *Drosophila* Shaker potassium channel, with the exception of the last amino acid (arginine in hKv1.5, threonine in Shaker).²⁹ Mutations on either end of the ion pore in Shaker alter the affinity for TEA (T441S for internal and T449Y for external TEA).⁴⁵ Internal TEA blocks Shaker K^+ channels with a voltage dependence described by an electrical distance of 0.15,⁴⁵ which suggests that TEA moves approximately 15% into the membrane electrical field. This value is similar to those previously described for quinidine ($\delta=0.18$),³¹ $R(+)$ - and $S(-)$ -bupivacaine ($\delta=0.16$),⁴¹ two enantiomers of a new benzazepin-2-*on* derivative with specific bradycardic effects ($\delta=0.19$),⁴⁶ and quinine ($\delta=0.18$)³⁶ and for zatebradine in the present experiments ($\delta=0.18$). All these findings may suggest the existence of a common receptor site for TEA, local anesthetics, and antiarrhythmic drugs both in Shaker and hKv1.5 channels. Moreover, the functional similarity between zatebradine-induced hKv1.5 block and that induced by TEA on Shaker channels, as well as the high structural similarity of the ion pores, would suggest that the T477 residue (equivalent of T441 Shaker) in hKv1.5 channels may be involved in zatebradine block. However, since zatebradine is a very hydrophobic molecule ($\log P=2.01$),⁴² we cannot rule out the possibility that other hydrophobic amino acids located in the pore of the channel also might be involved in the binding of zatebradine to hKv1.5 channels. Indeed, the residue at position 469 (Shaker B) within the S6 domain appears to contribute to the hydrophobic binding pocket for alkyl-TEA derivatives.⁴⁷ Variation of the hydrophobicity of this position by amino acid substitutions modulates the binding energy of the longer quaternary ammonium ions in a manner consistent with a direct hydrophobic interaction between the side chain of this residue and the alkyl tails of the blocker. Thus, the binding of zatebradine to the hKv1.5 channel pore could be similar to that of different alkyl-TEA compounds. Further studies with point mutations will help to test this hypothesis.

Clinical Implications

In isolated sinoatrial nodal cells, low concentrations of zatebradine (0.1 to $2 \mu\text{mol/L}$) reduced the diastolic depolarization rate and blocked the I_f in a use-dependent manner with an EC_{50} value of $0.5 \mu\text{mol/L}$ without causing a shift of its activation curve.¹⁵ However, in spontaneously beating sinoatrial nodal cells, rabbit Purkinje fibers, and guinea pig papillary muscles, zatebradine ($1 \mu\text{mol/L}$) also prolongs the action potential

▲ Top
▲ Abstract
▲ Introduction
▲ Methods
▲ Results
▪ Discussion
▼ References

duration.^{15 19 20} These results suggest that zatebradine exhibits additional class III effects and that the prolongation of the ventricular action potential duration must be due to the inhibition of an outward K^+ current different from the I_{Kr} present in rabbit sinoatrial myocytes.

In the present study, we have demonstrated that zatebradine blocks hKv1.5 channels in a concentration-, voltage-, time-, and use-dependent manner. Therefore, this effect on hKv1.5 channels could be the underlying mechanism by which zatebradine is able to prolong the action potential duration in sinoatrial node cells, papillary muscles, and Purkinje fibers.^{15 19 20} In the present experiments, the steady-state K_D value to block hKv1.5 channels was 1.8 $\mu\text{mol/L}$, which is less than four times higher than the value (0.5 $\mu\text{mol/L}$) for use-dependent inhibition of I_f in sinoatrial node cells.¹⁵ Moreover, we have also demonstrated that zatebradine-induced block of hKv1.5 channels was use dependent in such a way that at 0.5 and 1 Hz, zatebradine (10 $\mu\text{mol/L}$) inhibited the maximal peak hKv1.5 current by $\approx 40\%$, and this block persisted after 125-ms depolarizing pulses. Thus, it is possible that the reported steady-state K_D underestimates the potency of zatebradine to block hKv1.5 channels. Indeed, a recovery time constant of 1.5 seconds predicts that $\approx 60\%$ of steady-state block will be maintained at 1 Hz. Thus, a concentration as low as 0.5 $\mu\text{mol/L}$ would yield a 13% inhibition of the current by itself. The clinical relevance of the use- and frequency-dependent hKv1.5 block produced by zatebradine is currently unknown. The peak plasma levels found in healthy volunteers after intravenous and oral administration of zatebradine were 162 ± 71 ng/mL and between 24 and 35 ng/mL, respectively.^{13 14} Since zatebradine decreases I_f and heart rate in a use-dependent manner, it would be expected that the frequency-dependent block of hKv1.5 channels was progressively relieved as the heart rate was slowed. However, these pharmacokinetic studies were performed in healthy volunteers after the administration of zatebradine at doses different from those recommended in patients with coronary heart disease (2.5 to 7.5 mg twice a day).¹² Furthermore, the terminal half-life after oral administration was 2 to 3 hours, whereas the anginal and bradycardic effects of zatebradine persisted for >10 hours.¹² Because of the discrepancy between pharmacokinetic data and clinical efficacy, it was suggested that the tissular concentration rather than the plasma level of zatebradine is relevant.¹³ Under this assumption, the zatebradine-induced, use-dependent block of hKv1.5 channels could become of clinical relevance, since even at heart rates slower than the normal sinus rhythm (0.5 Hz), zatebradine is able to inhibit the hKv1.5-like current and thus prolong the action potential duration, probably with a K_D value similar to that necessary to inhibit the I_f in a use-dependent manner.

Moreover, the role of I_f in pacemaking is still controversial, and other factors, including activation of L- and T-type Ca^{2+} currents, the deactivation of delayed rectifier currents, a background Na^+ -dependent current, and the exchanger Na^+ - Ca^{2+} background current, also are expected to play an important role in pacemaker activity.^{48 49 50 51} Because the exact localization of hKv1.5 channels in the different regions of the heart is not known at the present time, we cannot rule out a potential role of these channels in modulation of pacemaker activity.

Acknowledgments

This study was supported by FIS grant 95/0318 (Dr Valenzuela), Salud 2000 grant (Dr Valenzuela), CICYT grant SAF92-0157 (Dr Tamargo), CAM grant 157/92 (Dr Tamargo), and NIH grant HL-47599 (Dr Snyders). The authors want to express their thanks to Dr M.M. Tamkun for providing us with the cell line transfected with the gene encoding hKv1.5 channels. We also thank G. Pablo and R. Vara for their excellent technical assistance. Zatebradine was kindly supplied by Dr Yves Joulin (Institut de Recherches Internationales Servier, Paris, France).

Selected Abbreviations and Acronyms

δ	= fractional electrical distance
f	= fractional block
hKv1.5	= human K^+ delayed rectifier current
I_{Ca}	= L-type Ca^{2+} current
I_f	= hyperpolarization-activated current
I_{Kr}	= rapid component of the delayed rectifier K^+ current
I_{Ks}	= slow component of the delayed rectifier K^+ current
I_{Kur}	= very rapidly activating delayed rectifier K^+ current
I_{to}	= transient outward current
I-V	= current-voltage
k	= association rate constant
K_D	= affinity constant

l	= dissociation rate constant
n_H	= Hill coefficient
pK_a	= negative log of equilibrium constant for dissociation
τ_B	= time constant of block
τ_{re}	= time constant of recovery from block
TEA	= tetraethylammonium

Received July 18, 1995; revision received December 18, 1995; accepted January 2, 1996.

References

1. Laurent D, Bolene-Williams C, Williams F, Katz N. Effects of heart rate on coronary flow and cardiac oxygen consumption. *Am J Physiol.* 1956;185:355-364.
2. Boudoulas H, Rittgers S, Lewis R, Leier C, Weissler A. Changes in diastolic time with various pharmacologic agents: implications for myocardial perfusion. *Circulation.* 1979;60:164-169. [[Medline](#)] [[Order article via Infotrieve](#)]
3. Hoffman J. Autoregulation and heart rate. *Circulation.* 1990;82:1880-1881. [[Free Full Text](#)]
4. Guth B, Heusch G, Seitelberger R, Ross J. Elimination of exercise-induced regional myocardial dysfunction by a bradycardic agent in dogs with chronic coronary stenosis. *Circulation.* 1987;75:661-669. [[Abstract/Free Full Text](#)]
5. O'Brien P, Drage D, Saeian K, Brooks H, Wartier D. Regional redistribution of myocardial perfusion by UL-FS49, a selective bradycardic agent. *Am Heart J.* 1992;123:566-574. [[Medline](#)] [[Order article via Infotrieve](#)]
6. Lillie C, Kobinger W. Investigations into the bradycardic effects of UL-FS 49 (1,3,4,5-tetrahydro-7,8-dimethoxy-3-[3-[[2-(3,4-dimethoxyphenyl)ethyl]methylimino]propyl]-2H-3-benzazepin-2-on hydrochloride) in isolated guinea pig atria. *J Cardiovasc Pharmacol.* 1986;8:791-797. [[Medline](#)] [[Order article via Infotrieve](#)]
7. Johnston W, Vinten-Johansen J, Tommasi E, Little W. ULFS-49 causes bradycardia without decreasing right ventricular systolic and diastolic performance. *J Cardiovasc Pharmacol.* 1991;18:528-534. [[Medline](#)] [[Order article via Infotrieve](#)]
8. Chen Z, Slinker B. The sinus node inhibitor UL-FS 49 lacks significant inotropic effect. *J Cardiovasc Pharmacol.* 1992;19:264-271. [[Medline](#)] [[Order article via Infotrieve](#)]
9. van Woerkens L, van der Giessen W, Verdouw P. The selective bradycardic effects of zatebradine (UL-FS 49) do not adversely affect left ventricular function in conscious pigs with chronic coronary artery occlusion. *Cardiovasc Drugs Ther.* 1992;6:59-65. [[Medline](#)] [[Order article via Infotrieve](#)]
10. Breall J, Watanabe J, Grossman W. Effect of zatebradine on contractility, relaxation and coronary blood flow. *J Am Coll Cardiol.* 1993;21:471-477. [[Abstract](#)]
11. Pistchner H, Muno E, Vens-Cappel F, Schulte B, Schlepper M, de Moura-Sieber V, Baiker W. Antiischemic, antianginal, and hemodynamic effects of ULFS 49 CI (a new heart-rate-reducing agent) in patients with angiographically proven CAD. In: Hjalmarson Å, Remme W, eds. *Sinus Node Inhibitors: A New Concept in Angina Pectoris.* New York, NY: Springer; 1991:45-53.
12. Baiker W, Czako E, Keck M, Nehmiz G. Efficacy and duration of action of three doses of zatebradine (ULFS 49 CI) in patients with chronic angina pectoris compared to placebo. In: Hjalmarson Å, Remme W, eds. *Sinus Node Inhibitors: A New Concept in Angina Pectoris.* New York, NY: Springer; 1991:55-63.
13. Franke H, Su CAPF, Schumacher K, Seiberling M. Clinical pharmacology of two specific bradycardic agents. *Eur Heart J.* 1987;8(suppl L):91-98.
14. Roth W, Bauer E, Heinzel G, Cornelissen P, van Tol R, Jonkman J, Zuiderwijk P. Zatebradine: pharmacokinetics of a novel heart-rate-lowering agent after intravenous infusion and oral administration to healthy subjects. *J Pharm Sci.* 1993;82:99-106. [[Medline](#)] [[Order article via Infotrieve](#)]

- ▲ [Top](#)
- ▲ [Abstract](#)
- ▲ [Introduction](#)
- ▲ [Methods](#)
- ▲ [Results](#)
- ▲ [Discussion](#)
- [References](#)

15. Goethals M, Raes A, van Bogaert P. Use-dependent block of the pacemaker current I_f in rabbit sinoatrial node cells by zatebradine (UL-FS 49). *Circulation*. 1993;88:2389-2401. [[Abstract/Free Full Text](#)]
16. van Bogaert P, Goethals M, Simoens C. Use- and frequency-dependent blockade by UL-FS 49 of the I_f pacemaker current in sheep cardiac Purkinje fibres. *Eur J Pharmacol*. 1990;187:241-256. [[Medline](#)] [[Order article via Infotrieve](#)]
17. van Bogaert P, Goethals M. Blockade of the pacemaker current by intracellular application of UL-FS 49 and UL-AH 99 in sheep cardiac Purkinje fibres. *Eur J Pharmacol*. 1992;229:55-62. [[Medline](#)] [[Order article via Infotrieve](#)]
18. Doerr T, Trautwein W. On the mechanism of the 'specific bradycardic action' of the verapamil derivative UL-FS 49. *Naunyn Schmiedebergs Arch Pharmacol*. 1990;341:331-340. [[Medline](#)] [[Order article via Infotrieve](#)]
19. Thollon C, Cambarrat C, Vian J, Prost J-F, Peglion J, Vilaine J. Electrophysiological effects of S 16257, a novel sino-atrial node modulator, on rabbit and guinea-pig cardiac preparations: comparison with UL-FS 49. *Br J Pharmacol*. 1994;112:37-42. [[Medline](#)] [[Order article via Infotrieve](#)]
20. Perez O, Gay P, Franqueza L, Carron R, Valenzuela C, Delpon E, Tamargo J. Electromechanical effects of zatebradine on isolated guinea pig cardiac preparations. *J Cardiovasc Pharmacol*. 1995;26:46-54. [[Medline](#)] [[Order article via Infotrieve](#)]
21. Wettwer E, Gath J, Hauser G, Mewes T, Reidemeister J, Ravens U. Transient outward current in human and rat ventricular cardiomyocytes. *Circulation*. 1992;86(suppl I):I-617. Abstract.
22. Beuckelmann D, Nabauer M, Erdmann E. Alterations of K^+ currents in isolated human ventricular myocytes from patients with terminal heart failure. *Circ Res*. 1993;73:379-385. [[Abstract/Free Full Text](#)]
23. Escande D, Coulombe A, Faivre J, Deroubaiz E, Coraboeuf E. Two types of transient outward currents in adult human atrial cells. *Am J Physiol*. 1987;252:H142-H148. [[Abstract/Free Full Text](#)]
24. Shibata E, Drury T, Refsum H, Aldrete V, Giles W. Contributions of a transient outward current to repolarization in human atrium. *Am J Physiol*. 1989;257:H1773-H1781. [[Abstract/Free Full Text](#)]
25. Wang Z, Fermini B, Nattel S. Delayed rectifier outward current and repolarization in human atrial myocytes. *Circ Res*. 1993;73:276-285. [[Abstract/Free Full Text](#)]
26. Jeck C, Boyden P. Age-related appearance of outward currents may contribute to developmental differences in ventricular repolarization. *Circ Res*. 1992;71:1390-1403. [[Abstract/Free Full Text](#)]
27. Boyle W, Nerbonne J. A novel type of depolarization-activated K^+ current in adult rat atrial myocytes. *Am J Physiol*. 1991;260:H1236-H1247. [[Abstract/Free Full Text](#)]
28. Wang Z, Fermini B, Nattel S. Sustained depolarization-induced outward current in human atrial myocytes: evidence for a novel delayed K^+ current similar to Kv1.5 cloned channel currents. *Circ Res*. 1993;73:1061-1076. [[Abstract/Free Full Text](#)]
29. Tamkun M, Knoth K, Walbridge J, Kroemer H, Roden D, Glover D. Molecular cloning and characterization of two voltage-gated K^+ channel cDNAs from human ventricle. *FASEB J*. 1991;5:331-337. [[Abstract](#)]
30. Snyders D, Tamkun M, Bennett P. A rapidly activating and slowly inactivating potassium channel cloned from human heart. *J Gen Physiol*. 1993;101:513-543. [[Abstract/Free Full Text](#)]
31. Snyders D, Knoth K, Roberds S, Tamkun M. Time-, state- and voltage-dependent block by quinidine of a cloned human cardiac channel. *Mol Pharmacol*. 1992;41:332-339.
32. Mays D, Foose J, Philipson L, Tamkun M. Localization of the Kv1.5 K^+ channel protein in explanted cardiac tissue. *J Clin Invest*. 1995;96:282-292.
33. Hondeghem L, Snyders D. Class III antiarrhythmic agents have a lot of potential, but a long way to go: reduced effectiveness and dangers of reverse use dependence. *Circulation*. 1990;81:686-690. [[Abstract/Free Full Text](#)]
34. Colatsky T, Follmer C, Starmer C. Channel specificity in antiarrhythmic drug action: mechanism of potassium channel block and its role in suppressing and aggravating cardiac arrhythmias. *Circulation*. 1990;82:2235-2242. [[Abstract/Free Full Text](#)]

35. Roden D. Current status of class III antiarrhythmic drug therapy. *Am J Cardiol.* 1993;72:44B-49B. [\[Medline\]](#) [\[Order article via Infotrieve\]](#)
36. Snyders D, Yeola S. Determinants of antiarrhythmic drug action: electrostatic and hydrophobic components of block of the human cardiac hKv1.5 channel. *Circ Res.* 1995;77:575-583. [\[Abstract/Free Full Text\]](#)
37. Valenzuela C, Delpon E, Perez O, Tamargo J, Snyders DJ. Effects of zatebradine on hKv1.5 channels. *Biophys J.* 1995;68:A36. Abstract.
38. Hamill O, Marty A, Neher E, Sakmann B, Sigworth F. Improved patch-clamp techniques for high resolution current recording from cells and cell-free membrane patches. *Pflugers Arch.* 1981;391:85-100. [\[Medline\]](#) [\[Order article via Infotrieve\]](#)
39. White M, Bezanilla F. Activation of squid axon K⁺ channels: ionic and gating current studies. *J Gen Physiol.* 1985;85:539-554. [\[Abstract/Free Full Text\]](#)
40. Valenzuela C, Sanchez-Chapula J, Delpon E, Elizalde A, Perez O, Tamargo J. Imipramine blocks rapidly activating and delays slowly activating K⁺ current activation in guinea pig ventricular myocytes. *Circ Res.* 1994;74:687-699. [\[Abstract/Free Full Text\]](#)
41. Valenzuela C, Delpon E, Tamkun M, Tamargo J, Snyders D. Stereoselective block of a human cardiac potassium channel (Kv1.5) by bupivacaine enantiomers. *Biophys J.* 1995;69:418-427. [\[Medline\]](#) [\[Order article via Infotrieve\]](#)
42. Snyders DJ, Bennett PB, Hondeghem LM. Mechanisms of drug-channel interaction. In: Fozzard H, Haber E, Jennings R, Katz A, eds. *The Heart and Cardiovascular System*. 2nd ed. New York, NY: Raven Press, Ltd; 1992:2165-2193.
43. Zagotta W, Aldrich R. Voltage-dependent gating of Shaker A-type potassium channels in *Drosophila* muscle. *J Gen Physiol.* 1990;95:29-60. [\[Abstract/Free Full Text\]](#)
44. Hille B. Local anesthetics: hydrophilic and hydrophobic pathways for the drug-receptor reaction. *J Gen Physiol.* 1977;69:497-515. [\[Abstract/Free Full Text\]](#)
45. Yellen G, Jurman M, Abramson T, MacKinnon R. Mutations affecting internal TEA blockade identify the probable pore-forming region of a K⁺ channel. *Science.* 1991;251:939-942. [\[Abstract/Free Full Text\]](#)
46. Delpon E, Valenzuela C, Perez O, Franqueza L, Gay P, Snyders D, Tamargo J. Mechanisms of block of a human cloned potassium channel by the enantiomers of a new bradycardic agent: S-16257-2 and S-16260-2. *Br J Pharmacol.* 1996;117:1293-1301. [\[Medline\]](#) [\[Order article via Infotrieve\]](#)
47. Choi K, Mossman C, Aube J, Yellen G. The internal quaternary ammonium receptor site of Shaker potassium channels. *Neuron.* 1993;10:533-541. [\[Medline\]](#) [\[Order article via Infotrieve\]](#)
48. Hagiwara N, Irisawa H, Kasanuki H, Hosoda S. Background current in sino-atrial node cells of rabbit heart. *J Physiol (Lond).* 1992;448:53-72. [\[Abstract/Free Full Text\]](#)
49. Shibata E, Giles W. Ionic currents which generate the spontaneous diastolic depolarizations in individual cardiac pacemaker cells. *Proc Natl Acad Sci U S A.* 1985;82:7796-7800. [\[Abstract/Free Full Text\]](#)
50. Campbell D, Rasmusson R, Strauss H. Ionic current mechanisms generating vertebrate primary cardiac pacemaker activity at the single cell level: an integrative view. *Annu Rev Physiol.* 1992;54:279-302. [\[Medline\]](#) [\[Order article via Infotrieve\]](#)
51. Anumonwo J, Jalife J. Cellular and subcellular mechanisms of pacemaker activity initiation and synchronization in the heart. In: Zipes D, Jalife J, eds. *Cardiac Electrophysiology: From Cell to Bedside*. Philadelphia, Pa: WB Saunders Co; 1995:151-164.

This article has been cited by other articles:



Investigative Ophthalmology & Visual Science

▶ HOME

G. C. Demontis, C. Gargini, T. G. Paoli, and L. Cervetto

Selective Hcn1 Channels Inhibition by Ivabradine in Mouse Rod Photoreceptors

Invest. Ophthalmol. Vis. Sci., April 1, 2009; 50(4): 1948 - 1955.

[\[Abstract\]](#) [\[Full Text\]](#) [\[PDF\]](#)

JOURNAL OF PHARMACOLOGY AND EXPERIMENTAL THERAPEUTICS

▶ HOME

L. Monassier, B. Manoury, C. Bellocq, J. Weissenburger, H. Grenay, D. Zimmermann, J.-D. Ehrhardt, P. Jaillon, I. Baro, and P. Bousquet

{sigma}2-Receptor Ligand-Mediated Inhibition of Inwardly Rectifying K⁺ Channels in the Heart

J. Pharmacol. Exp. Ther., July 1, 2007; 322(1): 341 - 350.

[\[Abstract\]](#) [\[Full Text\]](#) [\[PDF\]](#)

JOURNAL OF PHARMACOLOGY AND EXPERIMENTAL THERAPEUTICS

▶ HOME

S. E. Kim, H. S. Ahn, B. H. Choi, H.-J. Jang, M.-J. Kim, D.-J. Rhie, S.-H. Yoon, Y.-H. Jo, M.-S. Kim, K.-W. Sung, *et al.***Open Channel Block of A-Type, Kv4.3, and Delayed Rectifier K⁺ Channels, Kv1.3 and Kv3.1, by Sibutramine**

J. Pharmacol. Exp. Ther., May 1, 2007; 321(2): 753 - 762.

[\[Abstract\]](#) [\[Full Text\]](#) [\[PDF\]](#)

JOURNAL OF PHARMACOLOGY AND EXPERIMENTAL THERAPEUTICS

▶ HOME

A. Lagrutta, J. Wang, B. Fermini, and J. J. Salata

Novel, Potent Inhibitors of Human Kv1.5 K⁺ Channels and Ultrarapidly Activating Delayed Rectifier Potassium Current

J. Pharmacol. Exp. Ther., June 1, 2006; 317(3): 1054 - 1063.

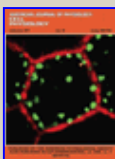
[\[Abstract\]](#) [\[Full Text\]](#) [\[PDF\]](#)

MOLECULAR PHARMACOLOGY

▶ HOME

J.-H. Lee, S. M. Jeong, J.-H. Kim, B.-H. Lee, I.-S. Yoon, J.-H. Lee, S.-H. Choi, D.-H. Kim, H. Rhim, S. S. Kim, *et al.***Characteristics of Ginsenoside Rg3-Mediated Brain Na⁺ Current Inhibition**

Mol. Pharmacol., October 1, 2005; 68(4): 1114 - 1126.

[\[Abstract\]](#) [\[Full Text\]](#) [\[PDF\]](#)

Am. J. Physiol: Cell Physiology

▶ HOME

B. H. Choi, J.-A. Park, K.-R. Kim, G.-I. Lee, Y.-T. Lee, H. Choe, S.-H. Ko, M.-H. Kim, Y.-H. Seo, and Y.-G. Kwak

Direct block of cloned hKv1.5 channel by cytochalasins, actin-disrupting agents

Am J Physiol Cell Physiol, August 1, 2005; 289(2): C425 - C436.

[\[Abstract\]](#) [\[Full Text\]](#) [\[PDF\]](#)

JOURNAL OF PHARMACOLOGY AND EXPERIMENTAL THERAPEUTICS

▶ HOME

H. Choe, Y.-K. Lee, Y.-T. Lee, H. Choe, S.-H. Ko, C.-U. Joo, M.-H. Kim, G.-S. Kim, J.-S. Eun, J.-H. Kim, *et al.***Papaverine Blocks hKv1.5 Channel Current and Human Atrial Ultrarapid Delayed Rectifier K⁺ Currents**

J. Pharmacol. Exp. Ther., February 1, 2003; 304(2): 706 - 712.

[\[Abstract\]](#) [\[Full Text\]](#) [\[PDF\]](#)



Journal of Cardiovascular Pharmacology and Therapeutics

[▶ HOME](#)

L. Sen, G. Cui, L.-M. Zhou, Y. Sakaguchi, and B. N. Singh
Acute Effects of Zatebradine on Cardiac Conduction and Repolarization

Journal of Cardiovascular Pharmacology and Therapeutics, March 1, 2002; 7 (1): 29 - 38.

[\[Abstract\]](#) [\[PDF\]](#)



JOURNAL OF PHARMACOLOGY AND EXPERIMENTAL THERAPEUTICS

[▶ HOME](#)

T. Gonzalez, M. Longobardo, R. Caballero, E. Delpon, J. Tamargo, and C. Valenzuela
Effects of Bupivacaine and a Novel Local Anesthetic, IQB-9302, on Human Cardiac K⁺ Channels

J. Pharmacol. Exp. Ther., April 13, 2001; 296(2): 573 - 583.

[\[Abstract\]](#) [\[Full Text\]](#)



JOURNAL OF PHARMACOLOGY AND EXPERIMENTAL THERAPEUTICS

[▶ HOME](#)

B. H. Choi, J.-S. Choi, S.-W. Jeong, S. J. Hahn, S. H. Yoon, Y.-H. Jo, and M.-S. Kim
Direct Block by Bisindolylmaleimide of Rat Kv1.5 Expressed in Chinese Hamster Ovary Cells

J. Pharmacol. Exp. Ther., May 1, 2000; 293(2): 634 - 640.

[\[Abstract\]](#) [\[Full Text\]](#)



Cardiovascular Research

[▶ HOME](#)

L. Yue, J. L. Feng, Z. Wang, and S. Nattel
Effects of ambasilide, quinidine, flecainide and verapamil on ultra-rapid delayed rectifier potassium currents in canine atrial myocytes

Cardiovasc Res, April 1, 2000; 46(1): 151 - 161.

[\[Abstract\]](#) [\[Full Text\]](#) [\[PDF\]](#)



Circulation

[▶ HOME](#)

R. Caballero, E. Delpon, C. Valenzuela, M. Longobardo, and J. Tamargo
Losartan and Its Metabolite E3174 Modify Cardiac Delayed Rectifier K⁺ Currents

Circulation, March 14, 2000; 101(10): 1199 - 1205.

[\[Abstract\]](#) [\[Full Text\]](#) [\[PDF\]](#)



Cardiovascular Research

[▶ HOME](#)

E. Delpon, C. Valenzuela, P. Gay, L. Franqueza, D. J. Snyders, and J. Tamargo
Block of human cardiac Kv1.5 channels by loratadine: voltage-, time- and use-dependent block at concentrations above therapeutic levels

Cardiovasc Res, August 1, 1997; 35(2): 341 - 350.

[\[Abstract\]](#) [\[Full Text\]](#) [\[PDF\]](#)

This Article

- [▶ Abstract FREE](#)
- [▶ Alert me when this article is cited](#)
- [▶ Alert me if a correction is posted](#)
- [▶ Citation Map](#)

Services

- [▶ Email this article to a friend](#)
- [▶ Similar articles in this journal](#)
- [▶ Similar articles in PubMed](#)
- [▶ Alert me to new issues of the journal](#)
- [▶ Download to citation manager](#)
- [▶ Request Permissions](#)

Citing Articles

- ▶ [Citing Articles via HighWire](#)
- ▶ [Citing Articles via Google Scholar](#)

Google Scholar

- ▶ [Articles by Valenzuela, C.](#)
- ▶ [Articles by Snyders, D. J.](#)
- ▶ [Search for Related Content](#)

PubMed

- ▶ [PubMed Citation](#)
- ▶ [Articles by Valenzuela, C.](#)
- ▶ [Articles by Snyders, D. J.](#)

[Circulation Home](#) | [Subscriptions](#) | [Archives](#) | [Feedback](#) | [Authors](#) | [Help](#) | [AHA Journals Home](#) | [Search](#)

Copyright © 1996 American Heart Association, Inc. All rights reserved. Unauthorized use prohibited.